Measurements of Water Vapor and High Clouds Over the Tibetan Plateau With the Terra MODIS Instrument

Bo-Cai Gao, Ping Yang, Guang Guo, Seon K. Park, Warren J. Wiscombe, and Baode Chen

***Abstract*—The seasonal variations of water vapor and cirrus clouds over the Tibetan Plateau are investigated using the recently available Level 3 monthly-mean atmospheric data products with a 1° × 1° latitude–longitude grid. The data products are derived from the multichannel imaging data acquired with the Moderate Resolution Imaging Spectroradiometer (MODIS) on the Terra Spacecraft. It is shown that the water vapor concentration over the Tibetan Plateau is normally low, whereas high clouds (mainly cirrus clouds) over the Plateau occur quite frequently. On an annual scale, the water vapor concentration reaches its maximum in July and its minimum in January. During the summer season, the southeastern part of Tibetan Plateau, which can be affected by moistures originating from the Bay of Bengal and southeastern Asia, is slightly moister than the other parts of the Plateau. This observation is in agreement with the previous surface meteorological measurements by Chinese scientists from the 1950s to mid-1970s. The mean high-cloud reflectance over the Plateau reaches its maximum in April and minimum in November. This feature of high clouds over the Plateau has not been reported previously. The special channel centered at 1.375-μm on the MODIS instrument has allowed the observation. We present a plausible mechanism to explain the seasonal variations of high clouds over the Plateau. We expect that the water vapor and high-cloud measurements with MODIS can be used to improve the model initialization and validation for climate models involving the Tibetan Plateau and the nearby regions in Asia.**

***Index Terms*—Cirrus clouds, meteorology, remote sensing, Tibetan Plateau, water vapor.**

I. Introduction

IT IS WELL KNOWN that the Tibetan Plateau, which has an average height of over 4 km and an area of about 2.4 million square meters, has profound thermal and dynamical influences on both local and global climate and atmospheric circulation [13], [22]–[25]. For examples, the Tibetan Plateau exerts major blocking effects on zonal and meridional air motions, resulting in strong horizontal and vertical perturbations of atmospheric flows. Tibet is one of the most intensive solar radiation regions in the world [11]. Its annual total amount of radiation at Mount Qomolangma (Everest) is 8332 MJ/m^2, only a little less than that in Poona (8583 MJ/m^2), India, and Cairo (8374 MJ/m^2), Egypt [6]. Due to the high elevations of the Tibetan Plateau, the air mass over it is only half of that over the adjacent low-level terrain. Thus, with the same amount of heat and water vapor, the corresponding temperature and humidity changes over the Tibetan Plateau are approximately twice of this in the lowlands [23]. The Tibetan Plateau as an elevated heat source in the summer significantly affects Asian summer monsoon circulation.

Cirrus clouds normally locate in the upper troposphere and lower stratosphere. They significantly modulate the flow of radiation budget by reflecting the incoming solar radiation, absorbing the thermal emission from the ground and the lower atmosphere, and reemitting infrared radiation into space. These clouds have been identified as one of the most uncertain components in the atmosphere [12], [18]. Observations indicate that thin cirrus clouds are ubiquitous [1], and much of the cirrus clouds in the atmosphere, especially in the tropics, are generated as the outflow or remains of cirroform anvils of cumulonimbus associated with deep convection [7]. Water vapor mainly concentrates below 4 km in the atmosphere, and is a major greenhouse gas. Its principle impact on the radiative balance of the earth is through longwave radiation. Knowledge of both water vapor and high-cloud properties and their variations in space and time is critical to understanding the thermal and dynamic effects of the Tibetan Plateau on the atmosphere.

In the past few decades, a number of investigations have focused on the dynamical, thermal, and radiation budget effects of the Tibetan Plateau on weather and climate [19], [20], [25]. From the 1950s to the mid-1970s and well before the era of "satellite meteorology," scientists in China [24] made some investigations on the distributions and properties of water vapor, clouds and aerosols, and their interactions with the atmosphere over Tibetan Plateau. These investigations were largely based on measurements from a very limited number of surface meteorological stations. The recently available satellite data from the Terra and Aqua Spacecrafts allow improved observations of water vapor and high-cloud distributions over Tibet.

Two Moderate Resolution Imaging Spectroradiometer (MODIS) instruments [9], [16] the first onboard the Terra platform launched on December 18, 1999 and the second onboard the Aqua platform launched on May 4, 2002, are uniquely designed, with a wide spectral range and a near daily global coverage, for remote sensing of the properties of land, ocean, and atmosphere, including column water vapor amount and high-cloud reflectances. Several channels in the

Manuscript received December 31, 2002; revised February 17, 2003. This research was supported by the NASA Goddard Space Flight Center and by the U.S. Office of Naval Research.

B.-C. Gao is with the Remote Sensing Division, Code 7212, Naval Research Laboratory, Washington, DC 20375 USA (e-mail: gao@nrl.navy.mil).

P. Yang and G. Guo are with the Department of Atmospheric Sciences, Texas A&M University, College Station, TX 77843 USA.

S. K. Park is with the Department of Environmental Science and Engineering, Ewha Womans University, Seoul, 120-750, Korea.

W. J. Wiscombe is with the Climate and Radiation Branch, NASA Goddard Space Flight Center, Greenbelt, MD 20771 USA.

B. Chen is with the Climate and Radiation Branch, NASA Goddard Space Flight Center, Greenbelt, MD 20771 USA and also with the Goddard Earth Sciences and Technology Center, University Maryland Baltimore County, Baltimore, MD 21250 USA.

Digital Object Identifier 10.1109/TGRS.2003.810704

near-infrared (NIR) spectral region were implemented on the MODIS for these purposes. Daily and seasonal variations of column atmospheric water vapor amounts have been observed reliably from MODIS channels located within and around the 0.94-μm water band [8]. Daily and seasonal variations of high clouds have also been observed from the 1.375-μm cirrus detecting channels [5]. In this letter, the seasonal variations and spatial distributions of water vapor and high clouds over the Tibetan Plateau and the possible formation mechanisms are studied using the data acquired with the MODIS instrument onboard the National Aeronautics and Space Administration Terra Spacecraft.

II. Descriptions of the MODIS Data

The MODIS instrument onboard the polar orbiting sun-synchronous Terra Spacecraft has 36 spectral channels between 0.4 and 14.3 μm. Among the 36 channels, several NIR channels located within and around the 0.94-μm water vapor band are used for remote sensing of column water vapor amounts. Column water vapor amounts or precipitable water vapor can be retrieved over clear land of the globe, and above clouds over both land and ocean. These channels are also useful for the retrieval of water vapor over extended oceanic areas with sun glint. The retrieval algorithm relies on observations of water vapor attenuation of NIR solar radiation reflected by surfaces and clouds. Techniques employing ratios of water vapor absorbing channels with the nearby atmospheric window channels at 0.865 and 1.24 μm are used [8]. The ratios partially remove the effects of variation of surface reflectance with wavelengths and results in the atmospheric water vapor transmittances. The column water vapor amounts are derived from the transmittances based on theoretical procedures. Water vapor values can be determined with errors typically in the range between 5% and 10%.

Thin cirrus clouds are traditionally difficult to detect by satellite sensors both in the visible and in the 10–12-μm infrared atmospheric window regions, particularly over land, due to their partial transparency and surface emission. Based on the analysis of hyperspectral imaging data collected by the Airborne Visible Infrared Imaging Spectrometer (AVIRIS) [21], it was found that the channel near 1.375 μm, where strong water vapor absorption occurs, is quite effective in detecting thin cirrus clouds [2], [4], [5]. This is due to the fact that, in the absence of cirrus clouds, little solar radiance scattered by the surface and lower clouds reaches an airborne or satellite sensor because of strong water vapor absorption in the lower atmosphere at this spectral band. When the high altitude cirrus clouds are present, the solar radiation scattered by these clouds can be received by the sensor. Based on the observation from AVIRIS data, a special channel centered at 1.375 μm was implemented on the MODIS instrument for remote sensing of cirrus clouds from space [3]. The algorithms [5], [8] for retrieval of column atmospheric water vapor amounts and high-cloud reflectances in the 0.4–1.0-μm spectral region have been developed and implemented for operational retrievals from MODIS data.

The MODIS data are generally processed into different levels from Level 1 (radiances or brightness temperatures that have been geolocated), to Level 2 (derived geophysical data products at the same resolution and location as the Level 1 data), to Level 3 (variables mapped onto uniform space-time grid scale) [10]. The MODIS atmospheric data products are now available for public access. The Level 2 water vapor and cirrus reflectance products are generated at the 1-km spatial resolution. Through integration of the Level 2 products, the Level 3 daily, eight-day, and monthly-mean water vapor products are generated globally at a $1^\circ \times 1^\circ$ latitude–longitude grid resolution. Because MODIS is the first satellite instrument with the capability of the 1.375-μm channel for cirrus detections, the Level 3 MODIS cirrus reflectance data product provides a unique opportunity to study cirrus clouds on regional and global scales and to improve the cirrus climatology. Table I lists the data products used in this study.

TABLE I
MODIS Data Products Used in This Analysis

Product	Quantities	Data Length
Atmospheric Monthly Global Joint Product (MOD08_M3) 1° by 1° resolution	Precipitable Water Vapor (cm)	Nov., 2000-Oct., 2002
Atmospheric Monthly Global Joint Product (MOD08_M3) 1° by 1° resolution	Cirrus Reflectance	Nov., 2000-Oct., 2002

III. Seasonal Variation of Water Vapor

The Tibetan Plateau is located in the region of 78°E $\sim$ 102°E, 26°N $\sim$ 38°N, surrounded by the earth's highest mountains, such as Great Himalaya Range, Pamir, Kunlun Mountains, and adjacent to the Indian subcontinent through the Himalayas. Fig. 1(A)–(D) shows the monthly-mean precipitable water vapor images over the latitude range of 10°N $\sim$ 55°N and the longitude range of 65°E $\sim$ 110°E for January [Fig. 1(A)], April Fig. 1(B)], July [Fig. 1(C)], and October [Fig. 1(D)] of 2002. The water vapor images are color coded so that red corresponds to 5 cm and blue 0 cm. The Tibetan Plateau is located in the center portions of the images. Due to the high elevations of the Tibetan Plateau, the water vapor values over the Plateau are much smaller than those over the surrounding low-elevation regions, such as the Indian subcontinent and Indo-China. There is a sharp boundary, which mainly includes Great Himalaya Range, Gongdise Mountains, Karakoram Range, and Pamir, between the Indian subcontinent and the Tibetan Plateau. The high mountains prevent most of the atmospheric water vapor over the Indian subcontinent from flowing into the Tibetan Plateau, and cause the largest moisture gradient across the boundary, particularly for the July image [Fig. 1(C)]. Through close examination of the Fig. 1(C) image, it can be seen that the southeastern part of the Tibetan Plateau ($\sim$ 28°N, 100°E) in the summer month is more moist than the other parts of the Plateau. This is because the moistures originating from the Bay of Bengal and southeastern Asia during summer can reach the southeastern part of the Plateau [24]. The spatial distributions of

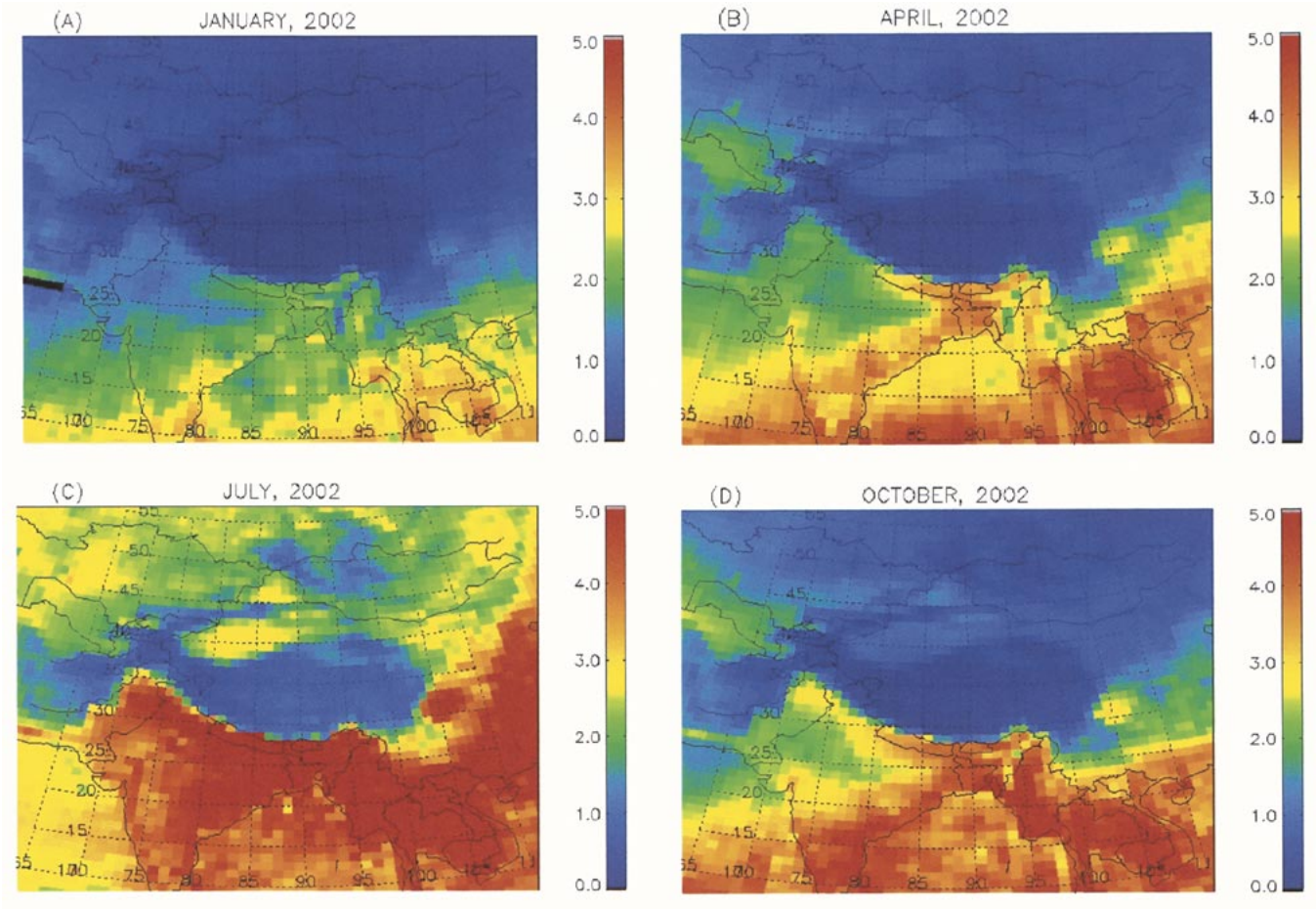

Fig. 1. MODIS Level 3 monthly-mean water vapor images over the Tibetan Plateau and the nearby Asian regions for (A) January, (B) April, (C) July, and (D) October of 2002.

water vapor over Tibet and Indian subcontinent are consistent with previous investigations [15], [17], [24], [26].

In order to have more quantitative descriptions on the seasonal variations of water vapor, we calculate the average values of water vapor over the Tibetan Plateau. In addition, we calculate the mean values of water vapor for the entire globe, a tropical belt between 30°N and 30°S, and a latitude belt near the equator between 10°N and 10°S. The simple mean value for water vapor concentration is computed via the following equation:

$$\overline{wv} = \frac{\sum_{1}^{n} w_i \cdot wv_i}{\sum_{1}^{n} w_i} \tag{1}$$

where $\overline{wv}$ is the mean water vapor value over a certain region, wv_i the pixel values over $1^\circ \times 1^\circ$ grid boxes for the same variable, and w_i the weighting factor ($w_i = 1$ for this case).

Fig. 2 presents Tibet mean (in the region of real Tibetan boundary), global mean, and the mean values over regions within the tropical belt and near the equator for 24 months from November of 2000 to October of 2002. Of the four sets of mean values over different spatial scales, the Tibetan mean values are the smallest whereas the mean values over the near-equator region are the largest. The two sets of mean values have almost

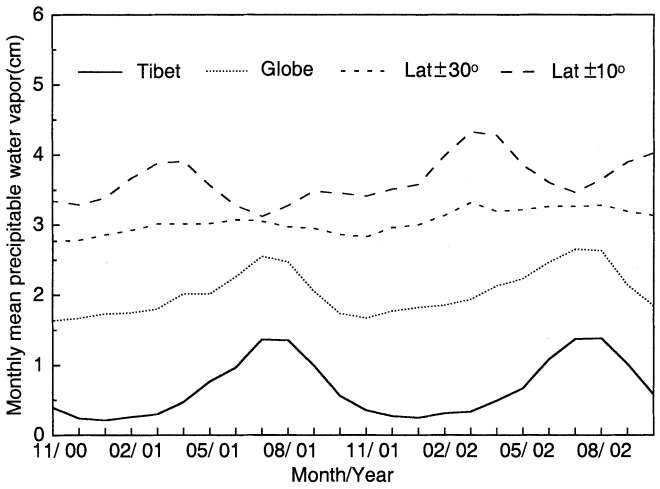

Fig. 2. Mean water vapor values over the Tibetan Plateau, the entire globe, a tropical belt between 30°N and 30°S, and a latitude belt near the equator between 10°N and 10°S.

the opposite seasonal tendency. The Tibetan mean values have the same seasonal variations as the globe mean values. For example, they reach their minimum in January (0.21 and 1.74 cm) or February (0.26 and 1.75 cm), and maximum in July (1.37 and 2.55 cm) or August (1.35 and 2.47 cm), respectively. However, the Tibetan mean values have larger magnitude of

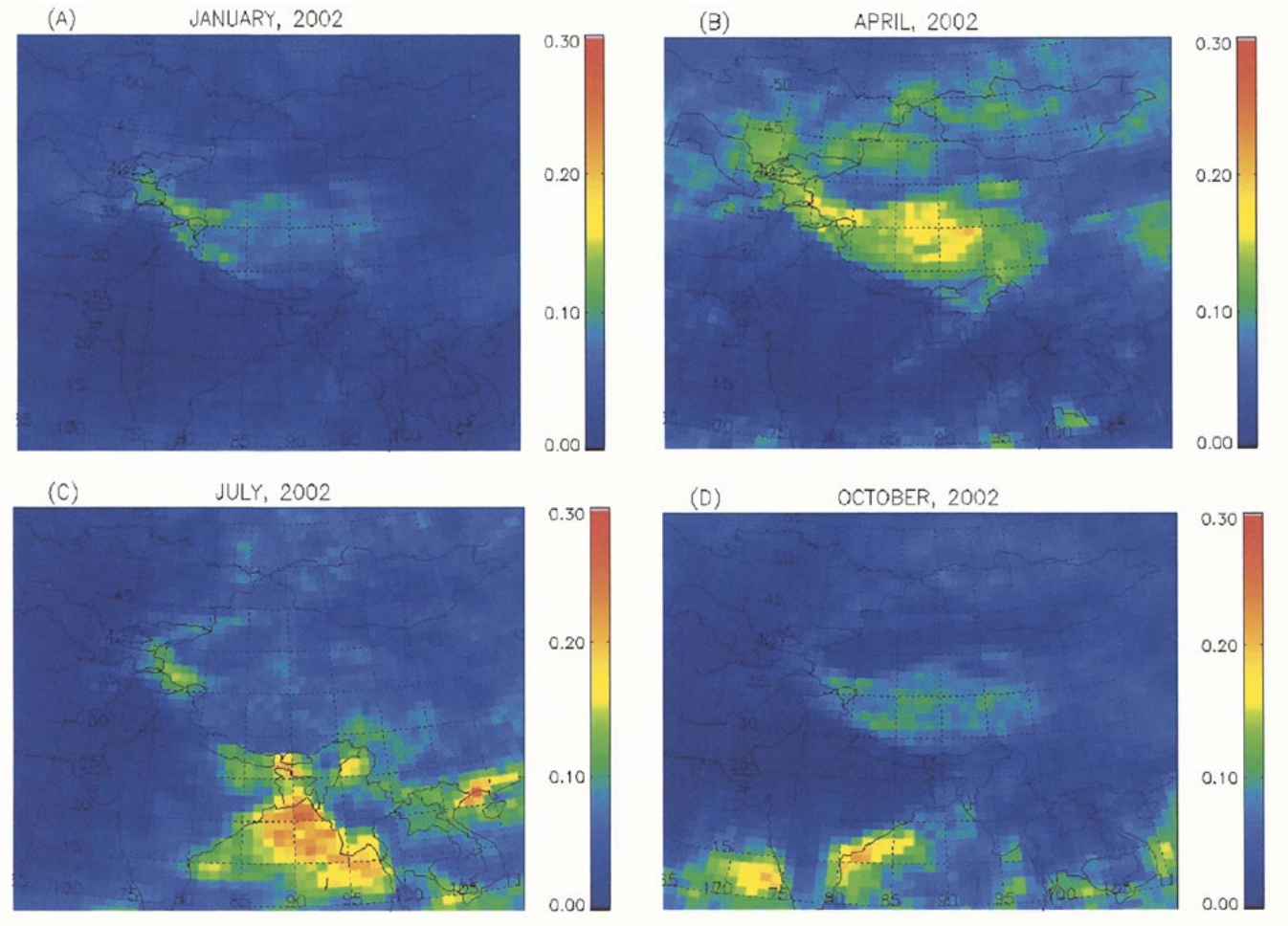

Fig. 3. MODIS Level 3 monthly-mean high-cloud reflectance images over the Tibetan Plateau and the nearby Asian regions for (A) January, (B) April, (C) July, and (D) October of 2002.

seasonal variations than the globe mean values. The mean values over the tropical belt (30°N to 30°S) have the smallest seasonal variation of the four. The results presented here are consistent with seasonal variations of the Plateau and global temperatures [13], and other studies [14], [15].

IV. Seasonal Variations of High Clouds

Fig. 3(A)–(D) shows the monthly-mean high-cloud reflectance images over the latitude range of 10°N ∼ 55°N and the longitude range of 65°E ∼ 110°E for January [Fig. 3(A)], April [Fig. 3(B)], July [Fig. 3C)], and October [Fig. 3(D)]of 2002. The images are color coded in such a way that red corresponds to a reflectance value of 0.3 and blue 0. For the Fig. 3(A) January image, a small amount of high clouds is seen over the Tibetan Plateau. Very few high clouds are seen over the Indian subcontinent (lower left) and the Indo-China regions (lower right). For the Fig. 3(B) April image (before the monsoon season), large amounts of high clouds with significant reflectance values are seen over the Tibetan Plateau. The high-cloud reflectances over the Indian subcontinent and Indo-China regions remain small. For the Fig. 3(C) July image, the high-cloud reflectances over the Tibetan Plateau decreased significantly in comparison with the April image. The high-cloud reflectances over the Bay of Bengal increased dramatically due to the solar heating of the water surfaces. As the evaporated water vapor from the ocean surfaces reaches the upper troposphere and lower stratosphere, cirrus clouds are formed after the air is cooled down near the tropopause. For the Fig. 3(D) October image, the high-cloud reflectances over the Tibetan Plateau increased slightly, while those over the Bay of Bengal decreased significantly in comparison with the July image.

Similar to our analysis of water vapor variations, we calculate the average high-cloud reflectances over the Tibetan Plateau, the entire globe, the tropical belt between 30°N and 30°S, and the latitude belt near the equator between 10°N and 10°S for 24 months from November 2000 to October 2002. The results are presented in Fig. 4. Contrary to water vapor curves shown in Fig. 2, the Plateau local mean value of high-cloud reflectance is the largest of the four. Moreover, this value has the largest seasonal variation and different seasonal tendency from the global mean value. For example, the maximum values of the Tibetan mean, which are 0.104 and 0.113 in both April 2001 and 2002, are twice as large as that of global means, 0.040 and 0.043, respectively. Meanwhile its minimum values, which are 0.055 in December 2000 and 0.050 in November 2001, are almost the

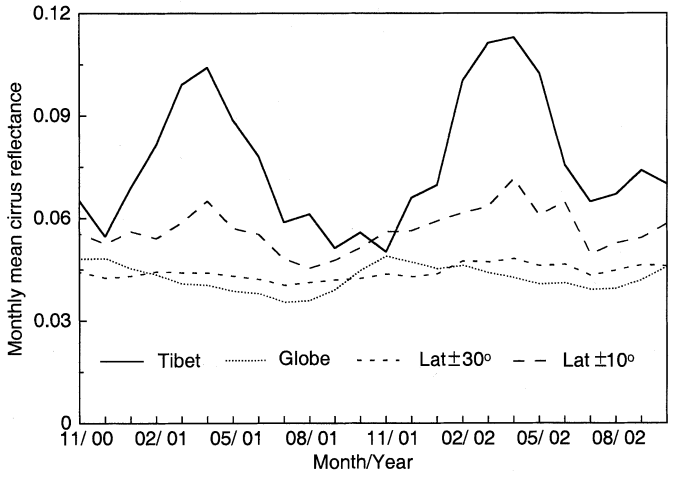

Fig. 4. Mean high-cloud reflectance values over the Tibetan Plateau, the entire globe, a tropical belt between 30°N and 30°S, and a latitude belt near the equator between 10°N and 10°S.

same as the corresponding global mean values of 0.048 and 0.049.

The maximum cirrus reflectances occur in April over the Tibetan Plateau, not in July when the Plateau receives the largest amount of solar radiation, as demonstrated in Figs. 3 and 4. Based on the general meteorology, surface conditions, and energy exchange mechanisms between the surface and the atmosphere over the Tibetan Plateau [24], we present a plausible mechanism to explain this phenomenon as follows. During April, the Hadley circulation in the India and Tibet regions is weak. There is little dry air from the stratosphere to sink over the Tibetan Plateau. April is the month near the end of the snow-melting season over the Plateau and before the beginning of the Indian monsoon season. There is a reasonable amount of water evaporation at the surface due to solar heating. Since the surface elevations of the Plateau are high ($>$ 4 km) and the surface pressures are low, the moist air can be quickly transported to the upper atmosphere through turbulent mixing, and high clouds, mainly cirrus clouds, are formed. During July, the sun moves further to the north, and the Hadley circulation over India and Tibet regions becomes stronger. There are significant amounts of dry air molecules from the stratosphere to sink over the Tibetan Plateau. Although the evaporation rates at the surfaces of the Plateau are increased due to the increased solar heating in July, the sinking dry air from the stratosphere prevents the moist air from reaching the tropopause. As a result, fewer high clouds are formed in July than in April over the Plateau.

V. Summary

We have studied the seasonal variations of water vapor and high clouds over the Tibetan Plateau using two years of the Terra MODIS Level 3 monthly-mean data products from November 2000 to October 2002. On an annual scale, the mean water vapor over the Plateau reaches its maximum in July and minimum in January. The southeastern part of the Plateau is slightly moister than the rest of the Plateau in the summer season. The observed seasonal variations of water vapor over the Plateau are consistent with those from previous investigations. MODIS is the first satellite instrument with the capability of 1.375-μm channel for remote sensing of high clouds from space. We have found that the mean of high-cloud reflectances over the Plateau reaches its maximum in April and minimum in November. The maximum does not occur in July—the peak solar heating month. We have presented a plausible mechanism to explain this observed phenomenon. The true mechanism may be different from the one we presented in this letter. More intensive meteorological and meteorological observation is needed to understand better the interactions between the land surface and the atmosphere over the Tibetan Plateau in the context of the Asian monsoon system. We expect that our understanding of meteorology over the Tibetan Plateau and the nearby Asian regions will be further improved in the future after the atmospheric information derived from MODIS data is used in climate models.

References

[1] H. Chepfer, P. Goloub, J. Spinhirne, P. H. Flamant, M. Lavorato, L. Sauvage, G. Brogniez, and J. Pelon, "Cirrus cloud properties derived from POLDER-1/ADEOS polarized radiances: First validation using a ground-based lidar network," *J. Appl. Meteorol.*, vol. 39, pp. 154–168, 2000.

[2] B.-C. Gao, A. F. H. Goetz, and W. J. Wiscombe, "Cirrus cloud detection from airborne imaging spectrometer data using the 1.38 μm water vapor band," *Geophys. Res. Lett.*, vol. 20, pp. 301–304, 1993.

[3] B.-C. Gao and Y. J. Kaufman, "Selection of the 1.375-μm MODIS channel for remote sensing of cirrus clouds and stratospheric aerosols from space," *J. Atmos. Sci.*, vol. 52, pp. 4231–4237, 1995.

[4] B.-C. Gao, Y. J. Kaufman, W. Han, and W. J. Wiscombe, "Correction of thin cirrus path radiance in the 0.4-1.0 μm spectral region using the sensitive 1.375 μm cirrus detecting channel," *J. Geophys. Res.*, vol. 103, pp. 32 169–32 172, 1998.

[5] B.-C. Gao, P. Yang, W. Han, R.-R Li, and W. J. Wiscombe, "An algorithm using visible and 1.38-μm channels to retrieve cirrus cloud reflectance from aircraft and satellite data," *IEEE Trans. Geosci. Remote Sensing*, vol. 40, pp. 1659–1668, Aug. 2002.

[6] Y. X. Gao, M. C. Tang, S. W. Luo, Z. B. Shen, and C. Li, "Some aspects recent research on the Qinghai-Xizang Plateau meteorology," *Bull. Amer. Meteorol Soc.*, vol. 62, pp. 31–35, 1981.

[7] R. A. Houze, Jr., *Cloud Dynamics*. San Diego, CA: Academic, 1993.

[8] Y. J. Kaufman and B.-C. Gao, "Remote sensing of water vapor in the near-IR from EOS/MODIS," *IEEE Trans. Geosci. Remote Sensing*, vol. 30, pp. 871–884, Sept. 1992.

[9] M. D. King, Y. J. Kaufman, W. P. Menzel, and D. Tanre, "Remote sensing of cloud, aerosol and water vapor properties from the Moderate Resolution Imaging Spectrometer (MODIS)," *IEEE Trans. Geosci. Remote Sensing*, vol. 30, pp. 2–27, Jan. 1992.

[10] M. D. King, W. P. Menzel, Y. J. Kaufman, D. Tanre, B.-C. Gao, S. Platnick, S. A. Ackerman, L. A. Remer, R. Pincus, and P. A. Hubanks, "Cloud and aerosol properties, and profiles of temperature and water vapor from MODIS," *IEEE Trans. Geosci. Remote Sensing*, pp. 442–458, Feb. 2003.

[11] Y. G. Kou *et al.*, "Solar radiation over the Qomolangma area. Explorative reports over the Qomolangma area during 1966–1968," in *Meteorology and Solar Radiation*. Beijing, China: Science Press, 1979.

[12] K. N. Liou, "Influence of cirrus clouds on weather and climate process: A global perspective," *Mon. Weather Rev.*, vol. 114, pp. 1167–1199, 1986.

[13] X. Liu and B. Chen, "Climatic warming in the Tibetan Plateau during recent decades," *Int. J. Climatol.*, vol. 20, pp. 1729–1742, 2000.

[14] X. Liu and Z.-Y. Yin, "Spatial and temporal variation of summer precipitation over the Tibetan Plateau and the North Atlantic oscillation," *J. Climate*, vol. 14, pp. 2896–2909, 2001.

[15] D. L. Randel, T. H. Vonder Haar, M. A. Ringeud, G. L. Stephens, T. J. Greenwald, and C. L. Combs, "A new global water vapor dataset," *Bull. Amer. Meteorol. Soc.*, vol. 77, pp. 1233–1246, 1996.

[16] V. V. Salomonson, W. L. Barnes, P. W. Maymon, H. E. Montgomery, and H. Ostrow, "MODIS: Advanced facility instrument for studies of the earth as a system," *IEEE Trans. Geosci. Remote Sensing*, vol. 27, pp. 145–153, Mar. 1989.

[17] V. P. Starr and J. P. Peixoto, "Hemisphere water vapor balance for the IGY," *Tellus*, vol. 4, pp. 463–472, 1965.
[18] G. L. Stephens, S.-C. Tsay, P. W. Stackhouse, and P. J. Flatau, "The relevance of the microphysical and radiative properties of cirrus clouds to climate and climate feedback," *J. Atmos. Sci.*, vol. 47, pp. 1742–1753, 1990.
[19] W. Su, J. Mao, F. Ji, and Y. Qin, "Outgoing longwave radiation and cloud forcing of the Tibetan Plateau," *J. Geophys. Res.*, vol. 105, pp. 14 863–14 872, 2000.
[20] Z. Sun, "Comparison of observed and modeled radiation budget over the Tibetan Plateau using satellite data," *Int. J. Climatol.*, vol. 15, pp. 423–445, 1995.
[21] G. Vane, R. O. Green, T. G. Chrien, H. T. Enmark, E. G. Hansen, and W. M. Porter, "The Airborne Visible/Infrared Imaging Spectrometer," *Remote Sens. Env.*, vol. 44, pp. 127–143, 1993.
[22] M. Yanai, C. Li, and Z. Song, "Seasonal heating of the Tibetan Plateau and its effects on the evolution of the summer monsoon," *J. Meteorol. Soc. Jpn.*, vol. 70, pp. 319–351, 1992.
[23] D. Ye, "Some characteristics of the summer circulation over the Qinghai-Xiznag (Tibet) Plateau and its neighborhood," *Bull. Amer. Meteorol. Soc.*, vol. 62, pp. 14–19, 1981.
[24] T.-D Yeh and Y.-X Gao, *Meteorology of Qinghai-Xizang (Tibet) Plateau*. Beijing, China: Science Press, 1979.
[25] Q. Zheng and K. N. Liou, "Dynamic and thermodynamic inferences of the Tibetan Plateau on the atmosphere in a general circulation model," *J. Atmos. Sci.*, vol. 43, pp. 1340–1354, 1986.
[26] P. Zhai and R. E. Eskridge, "Atmospheric water vapor over China," *J. Climate*, vol. 10, pp. 2643–2652, 1997.